ARTICLE

# Hypersonic Vibrations of $Ag@SiO_2$ (Cubic Core)−Shell Nanospheres

**Jing Ya Sun,[†] Zhi Kui Wang,[†] Hock Siah Lim,[†] Ser Choon Ng,[†] Meng Hau Kuok,[†,*] Toan Trong Tran,[‡] and Xianmao Lu[‡,*]**

[†]Department of Physics, National University of Singapore, Singapore 117542, Singapore, and [‡]Chemical and Biomolecular Engineering, National University of Singapore, Singapore 117576, Singapore

**ABSTRACT** The intriguing optical and catalytic properties of metal−silica core−shell nanoparticles, inherited from their plasmonic metallic cores together with the rich surface chemistry and increased stability offered by their silica shells, have enabled a wide variety of applications. In this work, we investigate the confined vibrational modes of a series of monodisperse $Ag@SiO_2$ (cubic core)−shell nanospheres synthesized using a modified Stöber sol−gel method. The particle-size dependence of their mode frequencies has been mapped by Brillouin light scattering, a powerful tool for probing hypersonic vibrations. Unlike the larger particles, the observed spheroidal-like mode frequencies of the smaller ones do not scale with inverse diameter. Interestingly, the onset of the deviation from this linearity occurs at a smaller particle size for higher-energy modes than for lower-energy ones. Finite element simulations show that the mode displacement profiles of the $Ag@SiO_2$ core−shells closely resemble those of a homogeneous $SiO_2$ sphere. Simulations have also been performed to ascertain the effects that the core shape and the relative hardness of the core and shell materials have on the vibrations of the core−shell as a whole. As the vibrational modes of a particle have a bearing on its thermal and mechanical properties, the findings would be of value in designing core−shell nanostructures with customized thermal and mechanical characteristics.

**KEYWORDS:** core−shells · vibrational modes · Brillouin light scattering · finite element simulations · mode displacement profiles

Core−shell nanoparticles have garnered intense interest due to their unique properties that have enabled applications in diverse areas such as catalysis, surface-enhanced Raman scattering (SERS), biosensing, bioimaging, and drug delivery.[1−10] Of particular interest are core−shell nanostructures derived from metal nanoparticles through coating with a silica layer. This is because such heteronanostructures have special catalytic, optical, and surface chemical properties derived from their metallic and silica components.[8−10] For instance, using gold−silica core−shell nanoparticles, Li *et al.* developed a new technique called shell-isolated nanoparticle-enhanced Raman spectroscopy which has a significantly higher detection sensitivity than existing surface- or tip-enhanced Raman spectroscopy.[8] The growth of silica shells on metal nanoparticles can be achieved using an approach adapted from the Stöber sol−gel method.[11,12] The key to this synthetic route is to attach a layer of functional ligands, such as (3-aminopropyl)trimethoxysilane, onto the metal nanoparticle surface followed by hydrolysis of the $-Si(OCH_3)_3$ groups to form the silica shell. Among the various metals employed as core materials, silver is of special significance in optical applications due to its strong surface plasmon resonance (SPR).[13,14]

However, most studies are confined to core−shell structures with spherical symmetry, while research into core−shells of other symmetries, such as those with faceted cores, is scarce.[7,9,15,16] Indeed, a major impediment to research into such nonspherical core−shells is the difficulty in synthesizing high-quality monodisperse core nanoparticles, especially those larger than 50 nm. However, due to their wide applications, recent years have seen the rapid development of synthetic techniques for producing nonspherical nanoparticles of various symmetries such as cubes, octahedra, triangular prisms, and other exotic shapes.[13,14,17−21] For instance, the large-scale synthesis of uniform-size silver nanocubes has been achieved by Im *et al.* following a polyol synthetic route.[19]

The confined acoustic vibrations of a freely oscillating particle are restricted to a set of discrete characteristic or eigenfrequencies. An understanding of these vibrational modes of a particle is essential to the calculation of its thermal properties such as the specific heat due to phonons.[22] While much research has been undertaken on the vibrational eigenmodes of single-component nanoparticles, little information is available on the eigenvibrations of

*Address correspondence to phykmh@nus.edu.sg, chelxm@nus.edu.sg.

Received for review September 29, 2010 and accepted November 3, 2010.

**Published online November 18, 2010.** 10.1021/nn102581g

hetero-nanoparticles.[23−28] This is particularly so for core−shells of nonspherical symmetry for which, to our knowledge, no study has been reported. Information on the dependence of core−shell eigenmodes on the shape of the core, thickness of the shell, and component materials is of fundamental scientific interest.

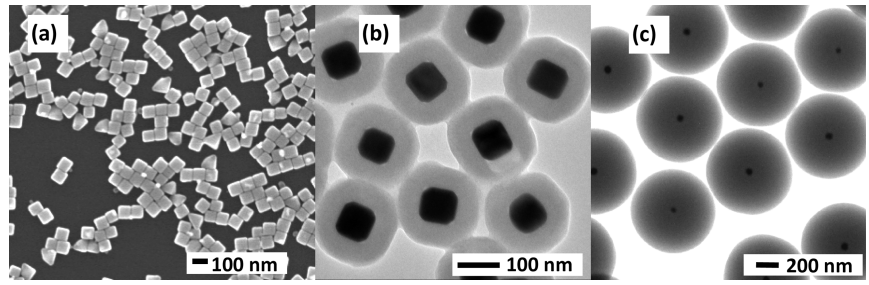


**Figure 1. (a) FESEM image of uncoated silver nanocubes of edge length $L$ = 76 nm. (b,c) TEM images of Ag@$SiO_2$ (cubic core)−shell nanospheres with respective diameters $D$ = 184 and 802 nm.**

In this article, we report on the first experimental study of the eigenvibrations of core−shell nanoparticles with nonspherical symmetry. For this study, monodisperse nanostructures in the form of silver cubic cores encased in silica spheres were fabricated using a modified Stöber sol−gel method for the first time. Brillouin light scattering, a powerful probe of hypersonic vibrational modes in the gigahertz range, was employed to map the particle-size dependence of the eigenfrequencies of a series of Ag@$SiO_2$ core−shells with a wide range of shell thicknesses. To elucidate the nature of the observed modes, numerical simulations based on the finite element approach were performed to determine the frequencies and displacement profiles. Additionally, to ascertain the influence of the material hardness of the core and shell on the vibrational mode frequencies, simulations were also carried out on the inverse structure, viz. $SiO_2$@Ag core−shells. The influence of the geometric shape of the core was also theoretically investigated.

## RESULTS AND DISCUSSION

Silver nanocubes, of edge length $L$ = 76 nm, stabilized with poly(vinylpyrrolidone) (PVP) were prepared in ethylene glycol following the method developed by Im *et al.*[19] The resulting silver nanocubes were then coated with silica using a modified procedure reported by Graf *et al.*[29] Briefly, an aqueous dispersion of the nanocubes with PVP was transferred into ethanol followed by mixing with water and ammonium hydroxide ($NH_4OH$). A solution of tetraethyl orthosilicate [$Si(OC_2H_5)_4$] in ethanol was then rapidly injected into the mixture. By varying the amount of water and the reaction time, core−shells with a wide range of silica shell thicknesses were synthesized. Upon completion of the growth of the silica shells, the particles were washed with ethanol and water several times and redispersed in water.

A series of six aggregates of monodisperse Ag@$SiO_2$ (cubic core)−shell nanospheres, with respective outer diameters $D$ = 148, 184, 204, 262, 392, and 802 nm, were used in this study. It is to be noted that the minimal possible outer core−shell diameter is 132 nm, the body diagonal of the $L$ = 76 nm cube, corresponding to the case where the shell just covers the entire cubic core. Characterization by field emission scanning electron microscopy (FESEM) and transmission electron microscopy (TEM) reveals that the nanoparticles are monodisperse and their shapes well-defined, as shown in Figure 1.

Prior to the Brillouin measurements, various aggregates of loose core−shell nanoparticles were prepared by eye dropping colloidal solutions of the nanoparticles onto respective clean pieces of silicon wafers, followed by vacuum drying at room temperature for several hours. All Brillouin spectra were excited by the 514.5 nm radiation from an argon ion laser and recorded in the 180° backscattering geometry using a 6-pass tandem Fabry−Perot interferometer.

The Brillouin spectra of the core−shells, which are generally well-resolved, feature several peaks. Representative spectra, displayed in Figure 2a−c, show that

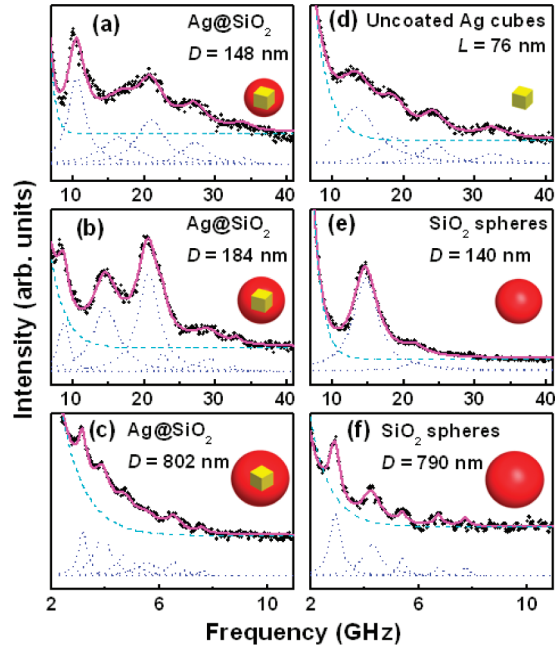


**Figure 2. (a−c) Brillouin spectra of Ag@$SiO_2$ (cubic core)−shell nanospheres with respective diameters $D$ = 148, 184, and 802 nm. (d) Brillouin spectrum of uncoated Ag nanocubes of edge length $L$ = 76 nm. (e,f) Brillouin spectra of homogeneous silica spheres with respective diameters $D$ = 140 and 790 nm. Experimental data are denoted by dots. The spectra are fitted with Lorentzian functions (dotted curves) and a background (dashed curves), while the resultant fitted spectra are shown as solid curves.**

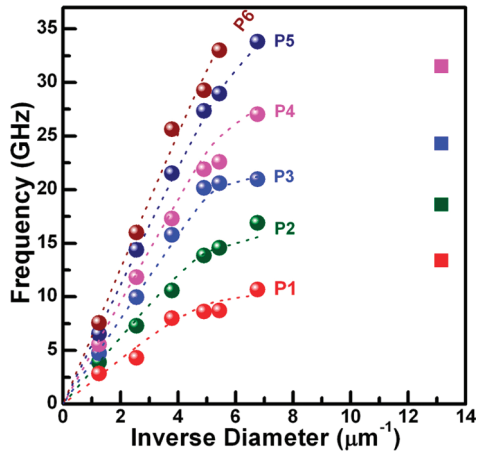


**Figure 3. Dependence of measured frequencies of Brillouin peaks, labeled as P1 to P6, of Ag@$SiO_2$ (cubic core)−shells on their inverse diameters (1/*D*). Experimental data on the core−shells are denoted by circular dots. Brillouin data, denoted by squares, on the uncoated Ag cubes of edge length *L* = 76 nm are also plotted against 1/*L*. The dotted lines are guides for the eye.**

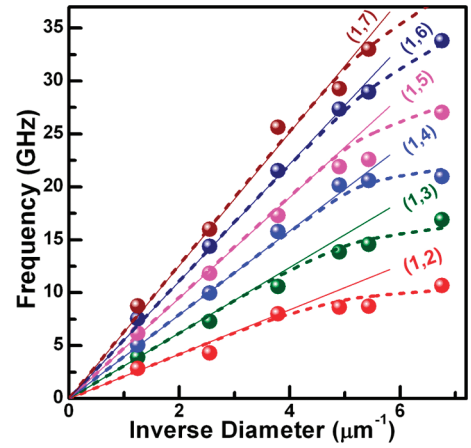


**Figure 4. Dependence of eigenmode frequencies of Ag@$SiO_2$ (cubic core)−shell nanospheres on their inverse diameter. Measured frequencies of Brillouin peaks are denoted by dots whose size represents measurement errors. Numerically calculated data are shown as dashed lines. The solid lines represent the theoretical frequencies of eigenmodes (*n*,*l*), based on Lamb's theory, of homogeneous $SiO_2$ spheres.**

each spectrum can be fitted with up to six Lorentzian peaks. The spectrum of the uncoated 76 nm silver nanocubes, shown in Figure 2d, contains four peaks, which were fitted with four Lorentzian curves. A comparison of Figure 2a and Figure 2d shows that the spectral features of $D = 148$ nm Ag@$SiO_2$ core−shells and those of uncoated silver nanocubes are different. This indicates that the presence of even a thin $SiO_2$ shell (≈8 nm thick, measured radially through a cube corner) can significantly affect the eigenvibrations of the nanocubes. It is noteworthy that the spectrum of the $D = 148$ nm core−shells also radically differs from that of solid homogeneous $SiO_2$ spheres with a similar size of $D = 140$ nm, which features only one dominant peak (Figure 2e). However, with increasing shell thickness, the spectral features of the Ag@$SiO_2$ heterostructures progressively resemble those of the homogeneous $SiO_2$ spheres of similar sizes. This is evident from a comparison of Figure 2c and Figure 2f, which shows the respective spectra of the $D = 802$ nm core−shells and the 790 nm $SiO_2$ spheres.

The frequencies of the six Brillouin peaks, labeled as P1, P2, P3, P4, P5, and P6, are plotted as a function of inverse core−shell particle diameter in Figure 3. Also displayed are the measured frequencies for the $L = 76$ nm bare silver cubes plotted against 1/*L*. Figure 3 reveals that as the size of the particles decreases from $D = 802$ nm, the peak frequencies are blue-shifted. The increase in the frequencies is steep for the larger particles but is more gradual for the smaller ones. It should be noted that, as stated above, the minimal possible core−shell diameter is 132 nm.

An earlier Brillouin study of homogeneous solid $SiO_2$ nanospheres established that their observed modes are spheroidal in nature, and that their eigenfrequencies are inversely proportional to their diameters,[24] confirming the theoretical prediction by Lamb.[30] In this theory, the modes are labeled by (*n*,*l*), where *l* denotes the angular momentum and *n* denotes the *n*th order solution for a given *l*. It is expected that as the Ag@$SiO_2$ nanosphere becomes larger, the effect of its fixed-sized core on the vibrational frequencies of the nanosphere as a whole will diminish. In other words, the larger core−shells will effectively behave as homogeneous solid $SiO_2$ nanospheres, as far as acoustic dynamics is concerned. Guided by this observation, we decided to compare the measured size dependence of the eigenfrequencies of the core−shells with the calculated size dependence of the eigenfrequencies $\nu_{nl}$ of homogeneous $SiO_2$ spheres, based on the Lamb theory. The calculations were performed following the procedure described in ref 25 and based on the respective Young modulus, Poisson ratio, and mass density values of 29 GPa, 0.18 and 1.96 g/cm$^3$ (corresponding to longitudinal and transverse sound velocities $V_L = 4009$ m/s and $V_T = 2505$ m/s, respectively) determined for $SiO_2$ nanospheres.[25] The calculated size dependences of the eigenfrequencies for the modes of $SiO_2$ spheres, labeled as ($n = 1$, $l = 2$), (1,3), (1,4), (1,5), (1,6), and (1,7) are shown as solid lines in Figure 4. It is to be noted that the spectral peaks observed by scattering from the core−shells are not assigned to the ($n = 1$, $l = 2$−7) spheroidal modes[31,32] of a homogeneous $SiO_2$ sphere.

Figure 4 shows that the calculated size dependence for the $SiO_2$ spheres (solid lines) is very close to the measured one for the larger Ag@$SiO_2$ core−shells. This observation, together with the similarity of the Brillouin spectra of the large core−shells and those of $SiO_2$ spheres of similar size, suggests that the observed peaks from the larger core−shells arise from eigenmodes which are spheroidal-like in character. Further, it can be deduced from these observations that the

presence of the $L = 76$ nm cores has a limited effect on the vibrational mode frequencies of core−shells when their size is much larger than that of the core.

To ascertain the acoustic dynamics of the core−shell particles, their eigenvibrations were computed using a numerical approach based on the finite element analysis technique. The displacement field $\boldsymbol{u}(\boldsymbol{r},t)$ of an elastic medium of density $\rho(\boldsymbol{r})$ is given by the following equations which govern small displacements $u_j$ of an elastic solid, and assuming the absence of body forces, can be expressed as

$$\rho \frac{\partial^2 u_j}{\partial t^2} = \frac{\partial}{\partial x_i}\left(C_{ikjl}\frac{\partial u_k}{\partial x_l}\right) \quad (1)$$

where $C_{ikjl}$ and $\rho$ are the stiffness tensor and material density, respectively. The equations, with the imposition of the stress-free boundary condition at the particle surface, were solved numerically using COMSOL Multiphysics[33] to yield the frequencies and displacement profiles of the eigenmodes.

In the numerical calculations, the same values of the elastic parameters, used above to determine mode frequencies of the silica sphere, were used for the silica shells.[25] In the case of the silver cores, the respective values of the Young's modulus, Poisson ratio, and density of 43 GPa, 0.43, and 10.5 g/cm$^3$ (corresponding to longitudinal and transverse sound velocities $V_L = 3415$ m/s and $V_T = 1196$ m/s, respectively), taken from ref 17, were used. Identification of the eigenmodes of the core−shells was carried out in the following way. The eigenmodes of the largest core−shell ($D = 802$ nm) were first calculated numerically. The resulting eigenfrequencies and displacement profiles were found to be very similar to those of the modes of a homogeneous $SiO_2$ sphere with the same diameter, which were also numerically computed. The six core−shell modes, whose frequencies and profiles match those of the (1,2) to (1,7) spheroidal modes of the $SiO_2$ sphere, were then identified as those giving rise to the six observed P1−P6 peaks of the core−shell. Hence, the observed modes of the core−shell are indeed spheroidal-like in nature. Figure 5 depicts the simulated profiles of the six spheroidal-like modes of the 802 nm core−shell. Eigenmodes of core−shells of other sizes were also numerically computed. Their P1−P6 modes were identified by comparing their profiles with the corresponding profiles of the 802 nm core−shell. The resulting eigenfrequencies are presented as dashed curves in Figure 4, which reveals that the simulated data accord very well with the Brillouin measurements. It is noteworthy that the displacement profiles of the particle with the thinnest shell ($D = 148$ nm) are very similar in resemblance to those of the 802 nm one.

It is evident that for the larger Ag@$SiO_2$ particles, the peak frequencies scale with inverse diameter (*i.e.*, $\nu \propto D^{-1}$), while the smaller ones exhibit a deviation from

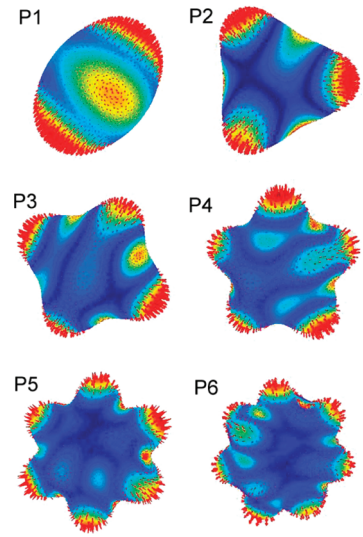


**Figure 5. Simulated displacement profiles of the various spheroidal-like vibrational modes of the $D = 802$ nm Ag@$SiO_2$ (cubic core)−shell nanospheres. The profiles are similar to those of the spheroidal modes of a homogeneous $SiO_2$ nanosphere, with respective angular momenta $l = 2$−7 for $n = 1$, corresponding to Brillouin peaks P1−P6 in Figure 3. The displacement magnitudes are color-coded, with red denoting the maximal value.**

this linear relationship. This deviation occurs for particles with diameters $D < 250$ nm (*i.e.*, $D^{-1} > 4$ μm$^{-1}$). Interestingly, the diameter at which the onset of the deviation occurs, $D_d$, is dependent on vibrational mode, decreasing with increasing mode energy. This can be explained qualitatively as follows. The displacement amplitudes of the higher-frequency vibrational modes are small, while those of the lower-frequency ones are larger. Hence, the vibrational energy of the former modes is expected to be confined mainly within the region below the surface of the core−shell sphere. In contrast, the lower-frequency modes have an energy distributed over a greater depth below the surface and are thus more sensitive to the presence of the core. It follows then that $D_d$ is larger for lower-frequency than for higher-frequency modes. This is an interesting phenomenon which warrants further theoretical investigation.

It would be of interest to explore the effects that the hardness of the component materials and the geometric shape of the core have on the vibrational mode frequencies of the core−shell structure. The influence of the material hardness is first investigated by carrying out simulations on the corresponding inverse core−shells, viz. $SiO_2$@Ag (cubic core)−shell nanospheres. Employing the above simulation procedure and material parameters for silver and silica, the respective frequencies of the lowest-energy spheroidal-like mode of the inverse core−shell and the lowest-energy (1,2) spheroidal mode of the homogeneous Ag nanosphere were calculated. The results are plotted as a function of inverse particle diameter (up to $1/D = 6.76$

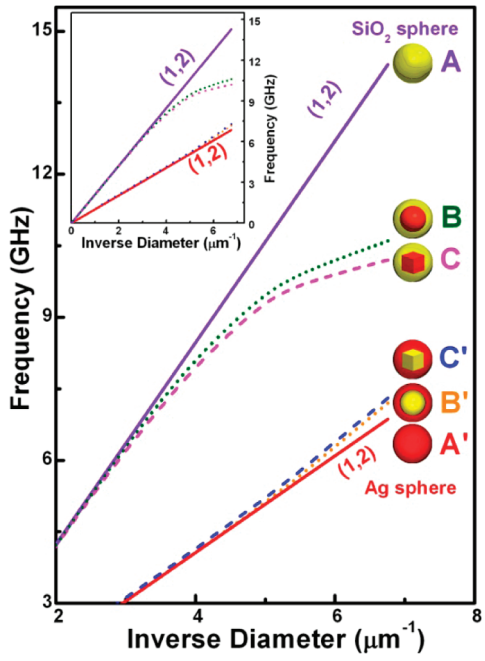


**Figure 6. Theoretical eigenmode frequencies of various nanoparticles as a function of inverse diameter. The six curves represent respective data for the (1,2) spheroidal modes of homogeneous $SiO_2$ spheres (solid violet line, A) and homogeneous Ag spheres (solid red line, A′); the lowest-energy spheroidal-like modes of Ag@$SiO_2$ spheres with a spherical core (dotted green line, B) or a cubic core (dashed pink line, C); the lowest-energy spheroidal-like modes of $SiO_2$@Ag spheres with a spherical core (dotted orange line, B′) or a cubic core (dashed blue line, C′). The cubic core (edge length = 76 nm) and the spherical core (diameter = 94.3 nm) have the same volume. The inset shows the complete calculated size dependence of the vibrational mode frequencies of the six series of particles.**

$\mu m^{-1}$, corresponding to our smallest $D$ = 148 nm) and shown respectively as C′ and A′ in Figure 6.

Like the Ag@$SiO_2$ (cubic core)−shell nanospheres (C), the eigenfrequencies of their inverse core−shells scale with $D^{-1}$ for the larger particles and deviate from this linear relationship for the smaller ones. However, instead of bending downward away from the linear line representing the (1,2) eigenmode of the $SiO_2$ homogeneous sphere (A), the "$\nu$ *vs* $D^{-1}$" curve of the inverse particles (C′) bends upward away from the linear line representing the (1,2) eigenmode of the Ag homogeneous sphere (A′). This can be understood from the fact that, as silica is harder than silver, the mode frequency of a silica particle is generally higher than that of a silver one of the same size and shape. It is noteworthy that the frequency deviation from linearity at $1/D = 6.76\ \mu m^{-1}$ is 40% for the direct core−shell, while it is only 6% for its inverse counterpart. This implies that, for a core−shell nanosphere comprising two given materials, a core composed of the softer material will have a stronger influence on the vibrational frequencies than one made of the harder material.

The effect of geometric shape was next investigated by considering Ag@$SiO_2$ and $SiO_2$@Ag nanospheres with a spherical core. The diameter of the core was set at $d$ = 94.3 nm, so that it has the same volume as the $L$ = 76 nm cubic core ($L^3 = \pi d^3/6$). The simulated size dependences of the lowest-energy mode frequencies of these Ag@$SiO_2$ and $SiO_2$@Ag structures are presented as B and B′, respectively, in Figure 6. Similar to the case of (cubic core)−shell nanospheres, the calculated eigenfrequencies of these spherical structures deviate from the "$\nu \propto D^{-1}$" linear relationship, for the smaller-sized structures. Our theoretical findings are borne out by the experimental data obtained by Still *et al.* in their studies of $SiO_2$@PMMA (hard core−soft shell)[27] and polystyrene@$SiO_2$ (soft core−hard shell)[28] spherical particles. Additionally, it is evident from Figure 6 that the deviation from linearity is less pronounced for particles with a spherical core than those with a cubic one (C and C′). This suggests that, for a core−shell composed of two given materials, a cubic core will have a greater impact on the core−shell vibrations than a spherical one, regardless of whether the core is composed of the harder or softer material.

## CONCLUSIONS

In summary, high-quality monodisperse core−shells, in the form of 76 nm silver cubes encased in silica nanospheres, have been fabricated by a modified Stöber sol−gel method. The vibrational modes of these core−shell particles were investigated using Brillouin light scattering. The frequencies of the observed modes, which were ascertained to be spheroidal-like in nature, were measured as a function of particle size. For the larger particles, the mode frequencies were found to scale with inverse diameter, but deviation from this linear relationship was observed for the smaller particles. Interestingly, the onset of this deviation occurs at a smaller particle size for higher-energy modes than for lower-energy ones. Finite element simulations reveal that the mode displacement profiles of the Ag@$SiO_2$ (cubic core)−shells closely resemble those of a homogeneous silica sphere. The experimental results were well reproduced by numerical calculations based on the finite element approach. Our simulations hint that, for a core−shell nanosphere of two given materials, a core composed of the softer material will have a stronger influence on the vibrational frequencies of the core−shell than a core made of the harder material. Additionally, a cubic core will have a greater impact on the core−shell vibrations than a spherical one, regardless of whether the core is made of the harder or softer material. As the thermal and mechanical properties of a particle are related to its vibrational modes, these findings would be of value in tailoring core−shell nanostructures with desired thermal and mechanical characteristics.

## MATERIALS AND METHODS

**Materials.** Ethylene glycol (EG, Sigma-Aldrich), silver nitrate ($AgNO_3$, Sigma-Aldrich), poly(vinylpyrrolidone) (PVP, MW = 55 000, Sigma-Aldrich), hydrochloric acid (HCl, 37%, Merck), ethanol ($C_2H_5OH$, Merck), tetraethyl orthosilicate ($Si(OC_2H_5)_4$, Sigma-Aldrich), and ammonium hydroxide ($NH_4OH$, Sigma-Aldrich) were used as received, and 18.2 MΩ · cm ultrapure water was used throughout the fabrication process.

**Synthesis of Ag Nanocubes.** In a typical synthesis, a glass vial containing 10 mL of EG was placed in an oil bath heated at 140 °C under stirring for 1 h. Then, 2.1 mL of HCl solution (3 mM, in EG) was then injected rapidly into the mixture. After 10 min, 6 mL of $AgNO_3$ (94 mM, in EG) and 6 mL of PVP (147 mM, in EG) were simultaneously pumped into the vial by using a two-channel syringe pump at a rate of 36 mL/h. The reaction vial was then capped and heated at 140 °C for 27.5 h, after which the product was washed with acetone and water several times to remove excess EG and PVP. The Ag nanocubes were finally redispersed in 16 mL of $H_2O$.

**Synthesis of Ag@$SiO_2$ Core−Shell Nanoparticles.** In a typical procedure, 0.1 mL of as-prepared Ag nanocubes, 1.077 mL of 85.5 mM PVP solution, and 0.9 mL of $H_2O$ were stirred vigorously in a glass vial for 12 h. The solution was then washed with $H_2O$ once to remove excess PVP in the solution and then transferred into ethanol. Subsequently, appropriate amounts of $H_2O$ and 45 μL of ammonium hydroxide ($NH_4OH$) were mixed with the reactant solution. A mixture of 70 μL of $Si(OC_2H_5)_4$ and 200 μL of ethanol was then rapidly injected into the reactant mixture. The reaction was stopped at desired reaction times, and the resulting core−shell nanoparticles were washed with ethanol and water. The concentrations of the reactants and reaction times are listed in Table 1. Finally, the Ag@$SiO_2$ nanoparticles were redispersed in water.

**TABLE 1.**

| core−shell diameter (nm) | $[NH_4OH]$ (M) | $[H_2O]$ (M) | $[Si(OC_2H_5)_4]$ (M) | reaction time (min) |
|---|---|---|---|---|
| 148 | 0.97 | 8.71 | 0.26 | 5 |
| 184 | 0.97 | 8.71 | 0.26 | 10 |
| 204 | 0.97 | 8.71 | 0.26 | 240 |
| 262 | 0.97 | 5.45 | 0.26 | 240 |
| 392 | 0.97 | 6.39 | 0.26 | 240 |
| 802[a] | 0.97 | 8.71 | 0.26 | 10; 120 |

[a]The coating step was performed twice for this sample.

**Brillouin Light Scattering.** All Brillouin measurements were performed at room temperature in the 180° backscattering geometry using a JRS Scientific Instruments (3 + 3)-pass tandem Fabry−Perot interferometer (FPI), of finesse about 120, equipped with a PerkinElmer SPCM-AQR-16 single photon counting (silicon avalanche diode) module. The 514.5 nm radiation of a Spectra Physics 2080−15S argon ion laser, operating in single mode, was used to excite the spectra. The power incident on the samples was of the order of a few milliwatts, and the data accumulation time for each spectrum ranges from 2 to 10 h.

*Acknowledgment.* This study was supported by the Ministry of Education Singapore, under Grants R-144-000-185-112 and R-279-000-273-133/298-112.

## REFERENCES AND NOTES


1. Zhang, J.; Tang, Y.; Lee, K.; Ouyang, M. Nonepitaxial Growth of Hybrid Core−Shell Nanostructures with Large Lattice Mismatches. *Science* **2010**, *327*, 1634–1638.
2. Alayoglu, S.; Nilekar, A. U.; Mavrikakis, M.; Eichhorn, B. Ru−Pt Core−Shell Nanoparticles for Preferential Oxidation of Carbon Monoxide in Hydrogen. *Nat. Mater.* **2008**, *7*, 333–338.
3. Tallury, P.; Payton, K.; Santra, S. Silica-Based Multimodal/Multifunctional Nanoparticles for Bioimaging and Biosensing Applications. *Nanomedicine* **2008**, *3*, 579–592.
4. Piao, Y.; Burns, A.; Kim, J.; Wiesner, U.; Hyeon, T. Designed Fabrication of Silica-Based Nanostructured Particle Systems for Nanomedicine Applications. *Adv. Funct. Mater.* **2008**, *18*, 3745–3758.
5. Shafer-Peltier, K. E.; Haynes, C. L.; Glucksberg, M. R.; Van Duyne, R. P. Toward a Glucose Biosensor Based on Surface-Enhanced Raman Scattering. *J. Am. Chem. Soc.* **2003**, *125*, 588–593.
6. Caruso, F. Nanoengineering of Particle Surfaces. *Adv. Mater.* **2001**, *13*, 11–22.
7. Levin, C. S.; Hofmann, C.; Ali, T. A.; Kelly, A. T.; Morosan, E.; Nordlander, P.; Whitmire, K. H.; Halas, N. J. Magnetic−Plasmonic Core−Shell Nanoparticles. *ACS Nano* **2009**, *3*, 1379–1388.
8. Li, J. F.; Huang, Y. F.; Ding, Y.; Yang, Z. L.; Li, S. B.; Zhou, X. S.; Fan, F. R.; Zhang, W.; Zhou, Z. Y.; Wu, D. Y.; *et al.* Shell-Isolated Nanoparticle-Enhanced Raman Spectroscopy. *Nature* **2010**, *464*, 392–395.
9. Joo, S. H.; Park, J. Y.; Tsung, C.-K.; Yamada, Y.; Yang, P.; Somorjai, G. A. Thermally Stable Pt/Mesoporous Silica Core−Shell Nanocatalysts for High-Temperature Reactions. *Nat. Mater.* **2009**, *8*, 126–131.
10. Liu, S.; Han, M.-Y. Silica-Coated Metal Nanoparticles. *Chem. Asian J.* **2010**, *5*, 36–45.
11. Stöber, W.; Fink, A.; Bohn, E. Controlled Growth of Monodisperse Silica Spheres in the Micron Size Range. *J. Colloid Interface Sci.* **1968**, *26*, 62–69.
12. Liz-Marzán, L. M.; Giersig, M.; Mulvaney, P. Synthesis of Nanosized Gold−Silica Core−Shell Particles. *Langmuir* **1996**, *12*, 4329–4335.
13. Jin, R.; Cao, Y.; Mirkin, C. A.; Kelly, K. L.; Schatz, G. C.; Zheng, J. G. Photoinduced Conversion of Silver Nanospheres to Nanoprisms. *Science* **2001**, *294*, 1901–1903.
14. Sun, Y.; Xia, Y. Shape-Controlled Synthesis of Gold and Silver Nanoparticles. *Science* **2002**, *298*, 2176–2179.
15. Xue, C.; Chen, X.; Hurst, S. J.; Mirkin, C. A. Self-Assembled Monolayer Mediated Silica Coating of Silver Triangular Nanoprisms. *Adv. Mater.* **2007**, *19*, 4071–4074.
16. Radi, A.; Pradhan, D.; Sohn, Y.; Leung, K. T. Nanoscale Shape and Size Control of Cubic, Cuboctahedral, and Octahedral Cu−$Cu_2O$ Core−Shell Nanoparticles on Si(100) by One-Step, Templateless, Capping-Agent-Free Electrodeposition. *ACS Nano* **2010**, *4*, 1553–1560.
17. Petrova, H.; Lin, C.-H.; de Liejer, S.; Hu, M.; McLellan, J. M.; Siekkinen, A. R.; Wiley, B. J.; Marquez, M.; Xia, Y.; Sader, J. E.; *et al.* Time-Resolved Spectroscopy of Silver Nanocubes: Observation and Assignment of Coherently Excited Vibrational Modes. *J. Chem. Phys.* **2007**, *126*, 094709.
18. Lu, X.; Rycenga, M.; Skrabalak, S. E.; Wiley, B.; Xia, Y. Chemical Synthesis of Novel Plasmonic Nanoparticles. *Annu. Rev. Phys. Chem.* **2009**, *60*, 167–192.
19. Im, S. H.; Lee, Y. T.; Wiley, B.; Xia, Y. Large-Scale Synthesis of Silver Nanocubes: The Role of HCl in Promoting Cube Perfection and Monodispersity. *Angew. Chem., Int. Ed.* **2005**, *44*, 2154–2157.
20. Nehl, C. L.; Liao, H.; Hafner, J. H. Optical Properties of Star-Shaped Gold Nanoparticles. *Nano Lett.* **2006**, *6*, 683–688.
21. Hao, E.; Bailey, R. C.; Schatz, G. C.; Hupp, J. T.; Li, S. Synthesis and Optical Properties of "Branched" Gold Nanocrystals. *Nano Lett.* **2004**, *4*, 327–330.
22. Chen, I.-C.; Weng, C.-L.; Tsai, Y.-C. Specific Heat of CdS/CdSe/CdS Quantum-Dot Quantum Wells. *J. Appl. Phys.* **2008**, *103*, 064310.
23. Li, Y.; Lim, H. S.; Ng, S. C.; Kuok, M. H.; Ge, M. Y.; Jiang, J. Z. Brillouin Study of Acoustic Phonon Confinement in $GeO_2$ Nanocubes. *Appl. Phys. Lett.* **2007**, *91*, 093116.

24. Kuok, M. H.; Lim, H. S.; Ng, S. C.; Liu, N. N.; Wang, Z. K. Brillouin Study of the Quantization of Acoustic Modes in Nanospheres. *Phys. Rev. Lett.* **2003**, *90*, 255502.
25. Lim, H. S.; Kuok, M. H.; Ng, S. C.; Wang, Z. K. Brillouin Observation of Bulk and Confined Acoustic Waves in Silica Microspheres. *Appl. Phys. Lett.* **2004**, *84*, 4182–4184.
26. Cheng, W.; Wang, J. J.; Jonas, U.; Steffen, W.; Fytas, G.; Penciu, R. S.; Economou, E. N. The Spectrum of Vibration Modes in Soft Opals. *J. Chem. Phys.* **2005**, *123*, 121104.
27. Still, T.; Sainidou, R.; Retsch, M.; Jonas, U.; Spahn, P.; Hellmann, G. P.; Fytas, G. The "Music" of Core−Shell Spheres and Hollow Capsules: Influence of the Architecture on the Mechanical Properties at the Nanoscale. *Nano Lett.* **2008**, *8*, 3194–3199.
28. Still, T.; D'Acunzi, M.; Vollmer, D.; Fytas, G. Mesospheres in Nano-Armor: Probing the Shape-Persistence of Molten Polymer Colloids. *J. Colloid Interface Sci.* **2009**, *340*, 42–45.
29. Graf, C.; Vossen, D. L. J.; Imhof, A.; van Blaaderen, A. A General Method To Coat Colloidal Particles with Silica. *Langmuir* **2003**, *19*, 6693–6700.
30. Lamb, H. On the Vibrations of an Elastic Sphere. *Proc. London Math. Soc.* **1882**, *13*, 189–212.
31. Montagna, M. Brillouin and Raman Scattering from the Acoustic Vibrations of Spherical Particles with a Size Comparable to the Wavelength of the Light. *Phys. Rev. B* **2008**, *77*, 045418.
32. Still, T.; Mattarelli, M.; Kiefer, D.; Fytas, G.; Montagna, M. Eigenvibrations of Submicrometer Colloidal Spheres. *J. Phys. Chem. Lett.* **2010**, *1*, 2440–2444.
33. *COMSOL Multiphysics*, Structural Mechanics, Manual, Comsol, AB, Stockholm, Sweden.